KONA Powder and Particle Journal

KONA Powder and Particle Journal No. 43 (2026) 269–280/https://doi.org/10.14356/kona.2026007 Original Research Paper

Using the Lubrication Approximation to Model the Effects of Viscosity in DEM Simulations for Complex Flow Regimes †

David N. de Klerk [1], Indresan Govender [1,2,3]*, Taswald L. Moodley [2,3] and Aubrey N. Mainza [1]

[1] *Department of Chemical Engineering, Centre for Minerals Research, University of Cape Town, South Africa*
[2] *Discipline of Chemical Engineering, School of Engineering, University of KwaZulu-Natal, South Africa*
[3] *Mintek, South Africa*

This study explores an efficient approach to modelling the flow of particles in wet granular systems using the Discrete Element Method (DEM). Typically, when particles move in a viscous fluid, DEM is coupled with Computational Fluid Dynamics (CFD) or Smooth Particle Hydrodynamics (SPH) methods to capture both particle and fluid motion. However, the computational expense and time required for one- or two-way coupled simulations, such as DEM–CFD or DEM–SPH, can be significant. In this research, a lubrication approximation is introduced to address fluid viscosity within DEM, which is particularly suitable for dense granular systems where viscous forces play a dominant role. DEM simulations incorporating the lubrication approximation were compared with *in situ* data obtained from Positron Emission Particle Tracking (PEPT) experiments. These experiments involve a cylindrical setup of radius $R = 230$ mm and length $L = 200$ mm, filled with 10 mm spherical glass beads at a 50 % fill fraction, and various mixtures of water and glycerol (60 %, 75 %, and 90 % by weight) as the fluid phase. Simulations are conducted within the LIGGGHTS–DEM framework, and detailed comparisons with PEPT data assess the suitability of the lubrication approximation for rotating drum systems. The analysis of tangential velocity profiles across different Stokes numbers reveals the applicability of the same constitutive equation for modelling both the PEPT and DEM data within a specified viscosity range, with the exception of the highest viscosity. This understanding is crucial for interpreting the flowing layer dynamics and optimising the simulation parameters for accurate predictions.

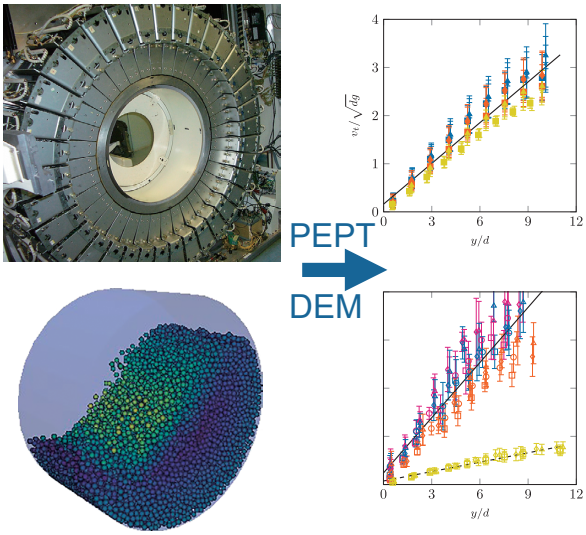

Keywords: lubrication, DEM, PEPT, granular rheology, viscosity

1. Introduction

Continuum numerical schemes exist for granular systems in the solid or gas-like states; however, there is no known continuum constitutive model for dense granular flows. While significant progress has been made in granular rheology, see Jop (2015) for a review, complex flows, such as two-dimensional flows in rotating drums, are still poorly understood (Cortet et al., 2009; Povall et al., 2021). In addition to the geometrical complexity, dense granular suspensions involve an interstitial fluid that fills the spaces between the solid material (Amarsid et al., 2017; Boyer et al., 2011; Pähtz et al., 2019; Trulsson et al., 2012).

The granular rheology of dense suspensions is an active area of study that relies heavily on efficient simulations of the particulate degrees of freedom to compare kinematic and dynamic quantities. In the absence of a continuum description, computer simulations of dense granular flows must be carried out at the scale of individual degrees of freedom. Such simulations are computationally expensive but provide a rich dataset that contains all physical quantities of each particle and the interactions thereof. The Discrete Element Method (DEM) is a numerical technique that simulates discrete particle behaviour in a granular medium (Cundall and Strack, 1979). Particle interactions are modelled as overlapping Hookean springs, where the degree of overlap is proportional to the repulsive forces. To prevent unrealistic collisional elasticity, a dashpot force based on the overlap velocity is invoked. Originally designed for dry particle systems, it can also be coupled with other techniques to model complex particle–fluid interactions. In such interactions, fluid layers between particles introduce forces such as inertia, viscosity, and pressure. Guo and

† Received 30 July 2024; Accepted 2 December 2024
J-STAGE Advance published online 19 April 2025
* Corresponding author: Indresan Govender;
[1] Add: P/Bag Rondebosch, 7701, South Africa
[2] Add: Durban, 4041, South Africa
[3] Add: P/Bag X3015, Randburg, Gauteng, 2121, South Africa
E-mail: indresan.govender@gmail.com
TEL: +27-83-274-9419

Curtis (2015) reviewed the application of DEM in modelling complex granular flows, including the effects of liquid-induced cohesion and lubrication. The importance of incorporating lubrication forces to improve model accuracy was emphasised, which is in line with the current study's focus on the effect of interstitial fluids. The Stokes number is a metric used to characterise the dominant force mechanisms induced by the fluid. Once understood, a suitable DEM-coupled framework can be selected. The Stokes number, given by

$$St = \frac{\rho_{\mathrm{p}} d^2 \dot{\gamma}}{\eta_{\mathrm{f}}}, \tag{1}$$

where ρ_{p} is the particle density, d the particle diameter, $\dot{\gamma}$ the shear rate and η_{f} the fluid viscosity, characterises the dominant force dynamics in coupled fluid–solid interactions. Such information can influence the choice of simulation conditions. In the case of low Stokes numbers, drag forces tend to dominate particle interactions, and it is feasible to simulate only the fluid (Xiao and Sun, 2011). On the other hand, at large Stokes numbers, particle momentum dominates, implying that considering lubrication effects in the fluid alone becomes feasible (Sun and Xiao, 2016). Naturally, one- or two-way coupled simulations may be considered for intermediate Stokes numbers.

When the Stokes regime is known in advance, computationally efficient one-way coupled simulations can be performed. Within this paradigm, fluid effects (e.g., drag and buoyancy) on particles are integrated into DEM as additional forces, whereas particle effects on fluids are disregarded (Malahe, 2012; Mayank et al., 2015).

At very high Stokes numbers, the computational efficiency can be further improved by eliminating the entire fluid phase simulation. Instead, the viscous effects arising from thin fluid films between particles are combined into a single lubrication force.

The normal and tangential components of the lubrication force exerted on particle j by particle i, represented by F_{ij}^{n} and F_{ij}^{t}, respectively, can be approximated by (Ball and Melrose, 1997; Cox, 1974):

$$F_{ij}^{\mathrm{n}}\left(h_{ij}\right) = \frac{3}{2}\pi\eta_{\mathrm{f}}\frac{d_{ij}^2}{h_{ij}}\left(v_i - v_j\right)\cdot n_{ij}n_{ij} \tag{2}$$

and

$$F_{ij}^{\mathrm{t}}\left(h_{ij}\right) = \frac{4}{5}\pi\eta_{\mathrm{f}}d_{ij}\times\left[1+\frac{d_{ij}}{d_i+d_j}+\left(\frac{d_i-d_j}{d_i+d_j}\right)^2\right]$$

$$\times\ln\left(\frac{d_{ij}}{2h_{ij}}\right)\left(v_i - v_j\right)\cdot\left(I - n_{ij}n_{ij}\right), \tag{3}$$

where h_{ij} is the gap between the particles, $d_{ij} = 2d_id_j/(d_i + d_j)$ is the effective grain diameter, and n_{ij} and t_{ij} are the normal and tangential unit vectors, respectively. The lubrication force depends on the proximity of particle i to particle j and activates when $h_{ij} < 0.05d_{ij}$. Increasing the proximity gap to $0.1d_{ij}$ has minimal effect on the outcome (Ness and Sun, 2015). The inherent nature of the equations may lead to numerical divergence when approaching the limit $\lim_{h_{ij}\to 0} F_{ij}^{\mathrm{t}}\left(h_{ij}\right) = \infty$. To address this issue, a strict lower limit of $h_{ij} = 0.001d_{ij}$ is enforced whenever $h_{ij} < 0.001d_{ij}$.

The effect of a fluid on the granular material can be modelled in several ways and has been reviewed by Peters et al. (2019), Wang et al. (2022), and Zhu et al. (2007, 2008). Although this work focuses on capturing the effect of viscosity using the lubrication approximation, a brief description of some key features and applicability of alternative methods is given.

The lubrication approximation is employed to model the hydrodynamic effects caused by shear forces between particles (Ball and Melrose, 1997; Cox, 1974; Kim and Karrila, 1991; Ness and Sun, 2015, 2016; Seto et al., 2013; Trulsson et al., 2012). These studies collectively reinforce the validity of using the lubrication approximation in DEM simulations to model granular flows, particularly in capturing the complex interactions and effects of interstitial fluids. Within this framework, the thickness of the fluid layers between particles is negligible compared to other dimensions of the system, such as particle size. By neglecting the inertial forces and pressure gradients, which are more pronounced in thicker fluid layers, this approximation simplifies the ensuing mathematics by considering only the viscous force. Furthermore, it is assumed that this viscous force occurs in a two-dimensional plane; therefore, the method does not capture three-dimensional flow effects like vortices and eddies found in complex fluid systems. In addition, the validity of the lubrication approximation can be affected by particle roughness and shape. Hence, this approach is well-suited for dense granular systems in which particles are in close contact and liquid films are thin, i.e., dense granular flows. The lubrication approximation is typically more accurate in laminar or low Reynolds number flows, where the fluid flow is smooth and well-ordered. However, in turbulent flows, thin liquid films can be disrupted, resulting in the formation of thicker regions or droplets. This approach has been successfully applied to studying various phenomena, including particle packing in concrete mortar (Cai, 2017) and understanding shear stress in dense fluid–grain mixtures (Marzougui et al., 2015).

Implementing the lubrication approximation within the DEM framework requires calculating the fluid film thickness; this is approximated using the Hertz–Mindlin model (Brilliantov et al., 1996; Silbert et al., 2003), which is a function of particle interactions. The shear rate, which controls the degree of shear flow and thus the viscous force within the fluid layer, is then computed based on the relative velocity between the DEM particles and fluid viscosity. A limitation arises when considering surface tension and viscosity because larger values of these properties may

result in undesirable capillary or drag forces. The lubrication force is subsequently computed based on the shear rate and liquid film thickness, which can be related using the Reynolds lubrication, Stokes, or Carman–Kozeny models (Bolton et al., 2005; Tichy, 1995); note that the Stokes model does not produce torque and therefore cannot predict particle rotation in shear flows (Apostolou and Hrymak, 2008). Finally, this lubrication force is added to the DEM particles as an additional term in the force balance, allowing for the inclusion of liquid film effects. Unfortunately, the method is limited to cases in which the resulting particle force has negligible influence on the fluid, i.e., no two-way coupling.

Liquid bridge modelling is an approach used to simulate the effects of viscosity in wet systems. The resultant liquid bridge represents the cohesive force resulting from capillary effects or liquid films. In liquid bridge modelling, liquid bridges are larger and more substantial than thin liquid films in the lubrication approximation. Although the cohesive forces between particles were captured, the influence of fluid flow properties such as the shear rate, turbulence, and pressure gradient on the liquid bridge were excluded. Calculating the liquid bridge force requires careful calibration of parameters like contact angle, liquid volume, and particle shape, some of which may be challenging to quantify (Washino et al., 2017). Although liquid bridge models have been embedded in DEM–CFD simulations by Kan et al. (2015) and Washino et al. (2013), these studies were computationally limited to small particle sets. Overall, the liquid bridge approach is particularly useful for studying wet systems in which cohesive forces dominate particle interactions (Gladkyy and Schwarze, 2014). Zhu et al. (2013) explored the effects of cohesion and lubrication in granular–fluid flows using liquid bridge-coupled DEM simulations. It was found that liquid bridge forces significantly affect flow dynamics by increasing the energy dissipated between colliding particles. These simulation results were validated against particle image velocimetry measurements.

To accurately capture and study other complex effects in particle–fluid systems, alternative modelling approaches are required. CFD methods, such as the Finite Volume Method or the Lattice Boltzmann Method (LBM), explicitly account for three-dimensional flow phenomena and provide a more comprehensive representation of fluid flow. These methods consider the full three-dimensional nature of the flow, yielding more accurate predictions than the simplified lubrication approximation, especially when the three-dimensional effects are significant, such as in complex flow patterns, turbulence, or near-wall interactions. The LBM uses a lattice-based velocity function to simulate fluid flow, and the resulting fluid forces are then applied to the DEM particles. The LBM, based on the kinetic Boltzmann equation, incorporates fluid–particle interactions at the mesoscale. The fluid viscosity in the LBM was controlled by the relaxation time parameter (τ) and lattice structure. The careful balancing of the lattice structure and τ is crucial for achieving stability and accuracy (Guo and Zhao, 2002). However, the limitation of this method lies in the boundary collision interaction between the solid and fluid. Various techniques, such as the Immersed Boundary Method (IBM), interpolation bounce back (IBB), and partial saturated method (PSM), have been proposed to address this issue. Chen et al. (2020) recently compared these treatments and concluded that the IBB method is the most accurate for realistic particle packing, whereas IBM is the most computationally demanding. Yang (2019) conducted a parametric study using the coupled Lattice Boltzmann Method and DEM to describe the dynamics of densely packed granular flows. It was highlighted that such models can capture complex interactions in granular systems, similar to the findings of the current study on the adequacy of lubrication approximation in high Stokes regimes.

In the CFD–DEM coupling approach, the fluid phase is modelled as a continuum using a CFD solver that numerically approximates the Navier–Stokes equations. Particles are modelled using DEM whilst the CFD solver accounted for the fluid viscosity, providing input for the DEM component of the simulation. The fluid properties, including viscosity, are then considered in the calculation of the forces and interactions between DEM particles. The information from the CFD solver is transmitted at each time increment to the DEM, which increases the computational complexity of the approach. Two-way coupled methods exist, where the momentum transfer from particles to the fluid is accounted for as well as the momentum transfer from fluid to particles (Kloss et al., 2012; Tanaka et al., 1993; Tsuji et al., 1993). To ensure robustness and stability, careful consideration must be given to the chosen modelling equations, mesh size–and time step. Due to its ability to capture fluid forces in greater detail, this method is applicable to a wide range of complex flows, including sediment transport, fluidised beds, and mixing processes (Hu et al., 1992; Sun and Xiao, 2016; Xiao and Sun, 2011).

CFD models the fluid phase in general; however, there may be instances where the wet system contains two or more immiscible fluid phases (e.g., free surface flows). In such systems, the Volume of Fluid (VOF) approach is preferred (Lin and Chen, 2013). The VOF approach splits each computational cell according to the volume fraction of the fluid. In doing so, the VOF approach has a distinct advantage over CFD in that it tracks interfacial boundaries. Unfortunately, this requires a significantly fine grid resolution, particularly at the fluid interfaces, to ensure accuracy. This is a prerequisite for providing information about each fluid phase in the computational domain. A similar outcome in CFD would require the use of CFD–IBM coupling, which is computationally demanding (El-Emam et al., 2021).

Smooth Particle Hydrodynamics (SPH) is a Lagrangian, meshless technique that numerically approximates an incompressible (or weakly compressible) version of the Navier–Stokes equations governing fluid flow (L iu and Liu, 2003). Potapov et al. (2001) and Cleary et al. (2006) described how SPH can be used to simulate the fluid phase of granular suspensions by adding particle-like degrees of freedom that simulate the fluid. SPH discretises the fluid into particles, each carrying properties such as position, velocity, density, and pressure, which govern their motion. These particles interact through a smoothing kernel function, and their influence is determined based on relative distances. The kernel function smoothes out properties of neighbouring particles, thereby allowing the calculation of various fluid properties within the domain. The continuum solution to the fluid is recovered by an averaging scheme over the new 'fluid' particles. By ensuring that the DEM particles are much larger than the SPH elements, fluid–solid interaction is achieved by placing the SPH elements inside their DEM counterparts. These interior SPH elements move and rotate with the solid DEM particles, initialised with the same density used for SPH elements representing the fluid phase. DEM–SPH coupling is suitable for systems where particle–fluid interactions are significant, such as sediment transport, granular flows in fluid, and fluidised bed simulations (Cleary et al., 2018a, 2018b).

This study investigates the use of the lubrication approximation to simulate dense granular suspensions in rotating drums. The numerical results will be validated against the experimental results. An experimental setup with comparable physical dimensions was used to measure particle kinematics using the Positron Emission Particle Tracking (PEPT) technique (Bemrose et al., 1988; Hawkesworth et al., 1986; Parker et al., 1993). The fluid is a mixture of water and glycerol, and the viscosity is modified by varying the ratio of the mixture.

The remainder of this paper is structured as follows: **Section 2** describes the computer simulations conducted in this work, and **Section 3** describes the experimental procedure used for validation, including the coarse-graining and analysis. **Section 4** presents the results, and **Section 5** presents the conclusions.

2. Numerical simulations

The LIGGGHTS (Kloss et al., 2012) DEM package was used for the numerical simulations. LIGGGHTS was developed as a standalone DEM extension to the popular molecular dynamics package LAMMPS (Plimpton, 1995). The simulations were performed in two stages: a particle generation simulation that served to create the initial condition and a continued simulation in which the drum's angular velocity and fluid viscosity were set to the desired values while relevant quantities were saved to disk for further processing.

2.1 Particle generation

This subsection describes the introduction of particles into the virtual rotating drum. The geometry of the system studied is a cylinder of radius $R = 230$ mm and length $L = 200$ mm. The cylinder with no lifter bars is imported into the simulation. The omission of lifter bars, which traditionally line the azimuthal surface, greatly simplifies the ensuing particle physics but also allows for undesirable particle slippage along this surface. Such a phenomenon is avoided by imposing particle–wall friction with coefficient $\mu = 0.5$. Gravity, which acts orthogonally to the drum's axis, is set to $g = 9.8$ m/s^2. The 10 mm diameter spherical glass beads (p) are defined with the following material properties: (i) Density $\rho_p = 2400$ kg/m^3, (ii) Young's modulus $Y = 5 \times 10^6$ kg/m/s^2, (iii) Poisson ratio $\nu = 0.45$, (iv) coefficient of restitution $e = 0.5$ and (v) coefficient of friction $\mu = 0.5$. To avoid computationally taxing particle interactions with the cylinder walls, particles are introduced into a horizontal cylindrical region slightly smaller than that of the drum. At random locations within this region, LIGGGHTS inserts 500 particles. Once inside, these particles experience gravitational forces and interactions resulting from overlapping particles according to the Hertz–Mindlin contact model. To prevent numerical instability arising from cases in which a newly created particle overlaps an existing particle, such particles are deleted upon creation. This process continues until 15,000 particles are detected in the system, representing 50 % drum filling on a volume basis.

2.2 Continued simulations

Leveraging LIGGGHTS' capability to save simulation states enables parametric studies of preset variables. After generating 15,000 particles, the simulation state was saved, and subsequent evaluations were performed based on the rotation rate and fluid viscosity, as outlined in **Table 1**. In LIGGGHTS, the rotation rate is defined by the rotation period (T), related to angular velocity (ω), Froude number (Fr), and critical speed (ω_c) as follows:

Table 1 Simulation parameters varied across the DEM study and the virtual simulation time (5–11 s) for each configuration. The drum rotation rate is given in RPM, angular velocity ω, as a percentage of the critical speed ω_c and Froude number (Fr). The relationships between these quantities are given by **Eqn. (4)**.

Rotation Speed				Viscosity (η_f) [Pa·s]			
RPM	ω [s^{-1}]	$\%\omega_c$	Fr	0.001	0.01	0.03	0.22
20.1	2.1	30	0.09	5 s	5 s	5 s	5 s
26.7	2.8	40	0.16	11 s	11 s	5 s	5 s
33.4	3.5	50	0.25	6 s	6 s	5 s	5 s
40.1	4.2	60	0.36	6 s	6 s	5 s	5 s

$$\omega = \frac{2\pi}{T}, \quad Fr = \frac{\omega^2 R}{g} \quad \text{and} \quad \omega_c = \sqrt{\frac{g}{R}} = 7.0/\text{s} \qquad (4)$$

To ensure a broad coverage of the Stokes number, a range of viscosities ($\eta_f \in \{0.01, 0.03, 0.22\}$ Pa·s) were selected. These viscosities correspond to Stokes numbers from $St \sim 10$ to $St \sim 100$. These viscosities were produced by diluting glycerol with water (60 %, 75 %, and 90 % by weight). The shear rate was estimated as $\dot{\gamma} \approx 20/\text{s}$ according to Govender et al. (2017).

In the simulation, a previously described lubrication force was applied exclusively to particle–particle contacts. Lubrication forces from wall–particle contacts were excluded for the following reasons: (i) **Eqns. (2)** and **(3)** depend on the diameter of both particles (d_{ij}), making extension interactions with flat walls (where $d_i \rightarrow \infty$) mathematically challenging. (ii) The LIGGGHTS code for particle–particle contacts could not be modified to account for particle–wall contacts, which was a practical constraint. (iii) Lubrication forces have minimal impact at the particle-wall interface, where particles are in direct contact with the wall, and these forces typically play a more influential role when there is a gap or fluid film between substrates.

The simulation advances at increments of $\Delta t = 1 \times 10^{-6}$ s over a period of 1,000,000 steps. The particle positions and velocities are saved to the disk every 0.01 s. The positions of particle–particle pairs that interact either through contact or lubrication forces are stored. **Fig. 1** shows a snapshot of the simulated spherical glass beads inside a rotating cylindrical drum.

Dell PowerEdge C6145 servers were used for simulations, with each simulation requiring between 27 and 30 h to complete a single simulated second. LIGGGHTS employs a 3D grid division of the simulation space, assigning particles within each grid division to the same processor.

The widely adopted Message Passing Interface (MPI) in high-performance computing facilitates LIGGGHTS' multi-core processing. Despite this, the open-source version lacks the capability to evenly distribute the computational workload across processors, i.e., it does not perform load balancing. Consequently, while LIGGGHTS partitions the simulation into 3D grids and assigns a unique processor to all particles in a given partition, these assignments remain fixed throughout the simulation. This static allocation results in an inherent imbalance in workload across processors because it is not dynamically adjusted.

The results of the present study revealed that simulations performed more efficiently without multi-processing. This observation can be attributed to the overhead introduced by inter-processor communication when assigning adjacent particles.

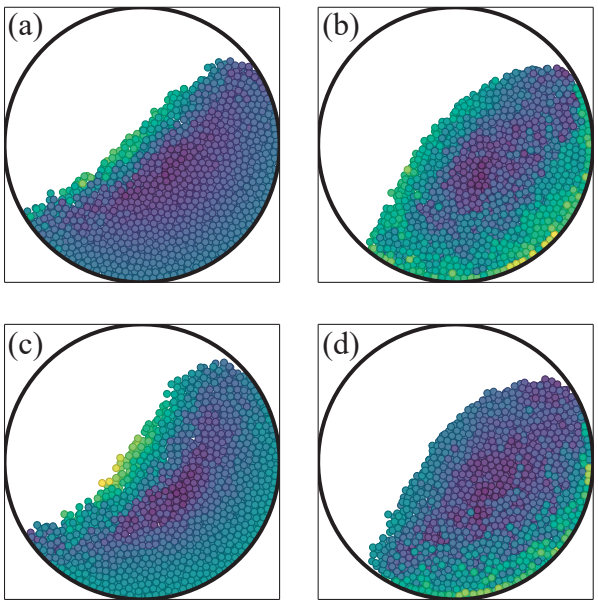

Fig. 1 Snapshots from various simulations of spherical glass beads inside the rotating cylindrical drum showing the distribution of particles for % ω_c and η_f **(a)** 30, 0.01 **(b)** 30, 0.22 **(c)** 60, 0.01 **(d)** 60, 0.22 (adapted with permission from De Klerk, 2019).

3. Experimental study

3.1 Particle kinematics

Positron Emission Particle Tracking (PEPT) is an *in situ* nuclear imaging technique (Bemrose et al., 1988; Hawkesworth et al., 1986; Parker et al., 1993) used to obtain the flow properties of particulate matter. Averaging these properties at the continuum scale enables high-resolution statistical validation of both rheological and numerical models (Govender et al., 2017; Moodley and Govender, 2022).

In general, PEPT relies on the activity of a radioactively labelled tracer particle within a bed of particles. The tracer's location is captured by a high-resolution Positron Emission Tomography (PET) scanner. To adhere to the Ergodic hypothesis (Wildmann et al., 2000), the experiment must run for an extended duration to ensure that the tracer traverses a significant portion of the phase space. This extended duration is crucial for determining confidence in the ensemble average.

Each data point obtained by PEPT has millimetre spatial and temporal resolutions. Consequently, the confidence is primarily determined from its kinematic outputs (velocity, solids fraction) at a continuum scale. Dynamic properties such as shear rate, pressure, and granular temperature, which are embedded in popular granular rheologies, are then computed from these kinematic values. To simplify subsequent physics, several scaling (Govender et al., 2017; Jop et al., 2005) and rheological studies have been necessarily restricted to slow-rotating drums (Chou and Lee, 2009; Orpe and Khakhar, 2001; Pignatel et al., 2012).

PEPT work was performed at the South African National Accelerator Centre, iThemba Laboratory for Accelerator Based Science (iThemba LABS). The EXACT3D (Model:

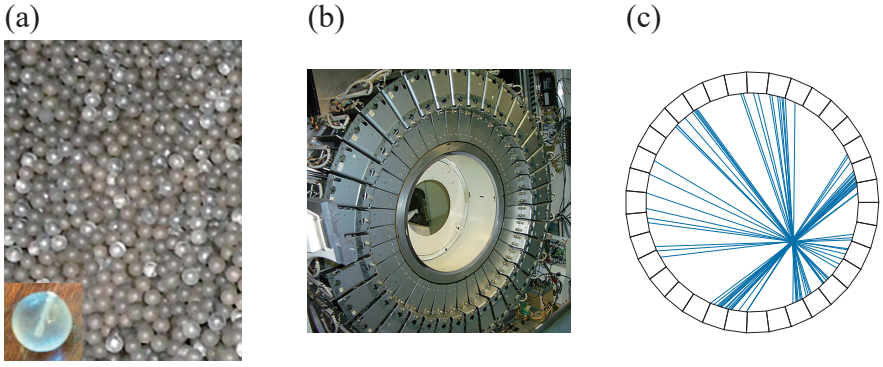

Fig. 2 **(a)** Glass beads as charge with tracer particles (insert bottom left) **(b)** PET camera **(c)** Lines of Response (LORs) (adapted with permission from De Kerk, 2019).

CTI/Siemens 966) PET scanner, consisting of 36 ×12 ×8 ×8 cylindrically orientated bismuth germanate (BGO) detector elements, is presented in **Fig. 2b**. Such an orientation allows particle tracking within a 50 cm-diameter field-of-view and 20 cm-deep field-of-view.

For this study, ^{68}Ga was selected as the radioactive source in the tracer particles because of its 68 min half-life, which provided ample time for data collection. In the case of radioactive contamination, quick mitigation is possible. The production of a tracer involves adsorbing ^{68}Ga into an ion-exchange resin (Cole et al., 2012). Choosing a resin with a specific gravity similar to that of glass helps prevent bias. This step ensures experimental uniformity and enhances the reliability of the results.

A high-density polyethylene cylinder with an inner radius of 230 mm and a length of 200 mm was used for conducting the experiments. Glass beads were introduced through a sidewall, which had four circular cutouts machined and resealed. A small port was incorporated to safely introduce the tracer (and thermocouple for temperature measurements) while minimising drum movement, which can be harmful during triangulation. Such temperature fluctuations at the completion of each 20 min run give rise to viscosity changes. The run time is limited to this time due to the file size limits of the acquisition system. To mitigate particle slippage along the azimuthal wall, a rubber lining with enhanced friction was introduced. The power draw was correlated using the torque sensor embedded in the variable-frequency drive of the drum motor. Hence, one can easily set the desired rotation rate and measure the resulting torque. Mono-sized glass beads (d = 10 mm) were made up to a 50 % drum filling by volume. Drum speeds were varied from 18.7 to 37.4 RPM, as indicated in **Table 2**.

Calibration is executed by placing a tracer at a specific point along the drum circumference. After tracking for 2 minutes, the circular path of the tracer was used to infer the drum position and orientation inside the PET scanner. This process ensures that the reference frame of the scanner is aligned with that of the drum. Once calibrated, each 20 minute run was conducted six to eight times. There is a limitation of a maximum of eight runs due to the tracer, which initially has an activity level of 1500 μCi, undergoing radioactive decay to a state where the data becomes unusable. Lower tracer activities often result in fewer recorded lines. In such cases, the triangulation algorithm fails to converge, and hence, the tracer must be replaced.

Table 2 Top: Drum speeds normalised by the critical speed, angular velocity, revolutions per minute and corresponding Froude number. The critical speed of the drum used in this study is ω_c = 6.35 rad/s = 62.3 RPM. Bottom: Fluid mixtures used together with each of the drum speeds in the table on the top. The viscosity of the mixture was calculated by Cheng (2008). The variation in viscosity was attributed to temperature fluctuations within the fluid.

ω/ω_c	ω [rad/s]	RPM	Fr
0.30	1.96	18.7	0.090
0.35	2.28	21.8	0.123
0.40	2.61	24.9	0.160
0.45	2.94	28.1	0.203
0.50	3.26	31.2	0.250
0.55	3.59	34.3	0.303
0.60	3.92	37.4	0.360

Water	Glycerol	Viscosity
% w/w	% w/w	Pa·s
40	60	0.011 ± 0.001
25	75	0.038 ± 0.005
10	90	0.25 ± 0.04

3.2 Fluid viscosity

Viscosity plays a crucial role in influencing the rheological behaviour of granular suspensions. Coussot et al. (2002) demonstrated that viscosity bifurcation (i.e., for smaller stresses, the viscosity increases and vice versa) occurs around a critical stress, influencing the transition between fluid and solid states. Cui et al. (2021) investigated

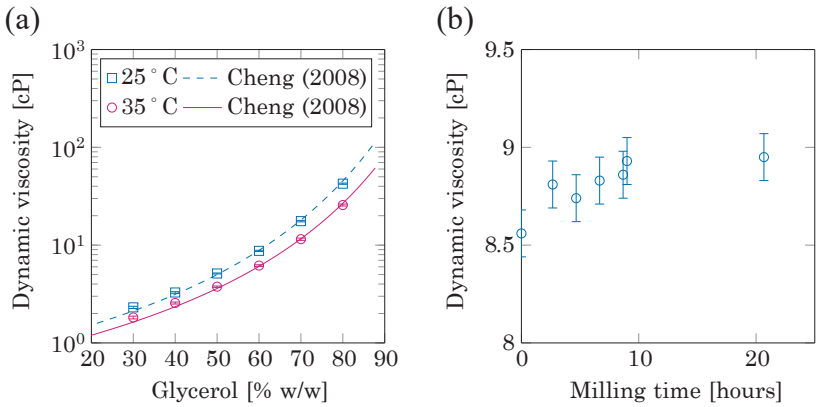

Fig. 3 **(a)** Measured viscosity of various water/glycerol mixtures compared to the parametrisation by Cheng (2008) at $T = 25$ °C and $T = 35$ °C and **(b)** viscosity fluctuation of a $T = 25$ °C 60 % w/w mixture over time (adapted with permission from De Klerk, 2019). The raw data are publicly available at J-STAGE Data (https://doi.org/10.50931/data.kona.28792256).

the effects of fluid viscosity on particle size segregation and found that increased viscosity decreased the segregation rate. Macaulay and Rognon (2021) used DEM to measure the viscosity of cohesive granular materials and established that adhesion-related numbers control the viscosity.

In the present study, the suspensive medium comprised mixtures of water and glycerol, with glycerol content ranging from 30 % to 80 % (w/w), as parameterised by Cheng (2008). These solutions were prepared by homogenising 180 g of glycerol and 45 g of water. To achieve the desired composition, 50 g of this mixture was replaced with 25 g of water, and this procedure was repeated six times.

Calibration against known solutions at temperatures $T = 25$ °C and $T = 35$ °C using a Brookfield DV-I viscometer ensured the accuracy of the prepared viscosities. **Fig. 3a** displays the results of measurements, comparing them to the parameterisation by Cheng (2008). The measured data correlate well with the parameterisation.

Throughout each experiment, the abrasion of glass beads led to temperature fluctuations and fine particle generation, causing changes in fluid viscosity. Consequently, the fluid viscosity was measured both before and after each PEPT run to ensure that it remained within an acceptable standard deviation. Based on **Fig. 3b**, where the measured viscosity at $T = 25$ °C is plotted against the residence time, the largely overlapping error bars imply that the viscosity was not adversely affected in the steady state.

3.3 Coarse graining

DEM provides high-fidelity dynamical data, such as stress and force, at microscopic resolution for each particle. Such detailed data are crucial for evaluating the rheological features of a system. The development of rheological models requires a continuum representation of the data. This involves transforming discrete pointwise data from the DEM into averaged values on a volume basis, a process known as coarse-graining. Classical statistical techniques underpin this approach; however, adaptation is needed for granular systems to address the scale separation effect, where particles are of the same order of magnitude as the averaging domain. In this context, the technique proposed by Artoni and Richard (2015), Babic (1997), and Glasser and Goldhirsch (2001) was employed to generate continuum fields. A brief description of this technique is provided below.

To determine the average value of a property ψ (such as force or power) at the centre of a given volume element (probe point $\vec{x}$ at time t), the following **Eqn. (5)** is used:

$$\rho(\vec{x},t)\psi(\vec{x},t) = \int \mathrm{d}t' \sum_p m_p \psi_p w_p = \int \mathrm{d}t' \sum_p m_p \psi_p K(\vec{x}-\vec{x}_p, t-t_p, W) \tag{5}$$

Here, subscript p refers to neighbouring particle properties at their centroid, with m_p representing the mass of the p^{th} neighbouring particle. The Gaussian smoothing kernel K assigns a normalised weighting factor w_p based on the displacement between the neighbouring particle and the probe point in both space $(\vec{x}-\vec{x}_p)$ and time $(t-t_p)$. The smoothing radius W ensures exclusion of particles beyond a certain distance $|\vec{x}-\vec{x}_p|$ from the probe point $\vec{x}$ in the current calculation.

The average density at the probe point, $\rho(\vec{x},t)$, is computed using **Eqn. (6)**:

$$\rho(\vec{x},t) = \int \mathrm{d}t' \sum_p m_p w_p \tag{6}$$

The selection of a continuous and differentiable smoothing kernel K allows the calculation of the gradient of property ψ in **Eqn. (5)** using the product rule (Artoni and Richard., 2015), as shown in **Eqn. (7)**:

$$\rho\nabla\psi = \int \mathrm{d}t' \sum_p (\nabla w_p) m_p \psi_p - \psi \int \mathrm{d}t' \sum_p (\nabla w_p) m_p. \tag{7}$$

Adapting **Eqns. (5)** and **(6)** to the PEPT data requires a slight adjustment to account for the Lagrangian nature of the measurement. Assuming the ergodic hypothesis (Wildmann et al., 2000), the summation terms in each equation can be modified for a tracer particle repeatedly traversing the phase space as follows:

$$\rho(x,t) \approx N \int \mathrm{d}t' m_\mathrm{T} K(x - x_\mathrm{T}, t - t_\mathrm{T}), \tag{8}$$

$$\rho(x,t)\psi(x,t) \approx N \int \mathrm{d}t' m_\mathrm{T} \psi_\mathrm{T} K(x - x_\mathrm{T}, t - t_\mathrm{T}) \tag{9}$$

where x_T is the position of the tracer at time t_T, and ψ_T is a particle property.

4. Results

The distribution of particles in some simulations is shown in **Fig. 1**. The analysis performed in this study focused on two primary objectives: (i) the applicability of the same constitutive equation to model both measured (PEPT) and simulated (DEM) data, and (ii) the associated viscosity effects. Govender et al. (2017) and Jop et al. (2005) established scaling relations for the velocity profile based on the constitutive equation $\tau/P = \mu(I)$ through a continuum force balance in the flowing layer. The resulting shear rate as a function of the flowing layer depth (y) led to the scaled velocity–depth relationship $v_\mathrm{t} / \sqrt{gd}$. The validity of the constitutive equation hinges on the statistical equivalence of this scaling relation between PEPT and DEM. **Fig. 4** (De Klerk, 2019) evaluates the scaled tangential velocity, $v_\mathrm{t} / \sqrt{dg}$, at various points along perpendicular slices of the flowing layer. The correlation between PEPT and DEM is well-established for viscosities up to 0.03 Pa·s, as evidenced by the linear least squares regression equations, and their high R^2 values are given by **Eqns. (10)**, **(11)**, and **(12)**:

$$\frac{v_\mathrm{t}}{\sqrt{dg}} = 0.282\left(\frac{y}{d}\right) + 0.161 \quad (R^2 = 0.949)\ \textit{all PEPT} \tag{10}$$

$$\frac{v_\mathrm{t}}{\sqrt{dg}} = 0.382\left(\frac{y}{d}\right) + 0.241$$

$$(R^2 = 0.861)\ \textit{DEM}\,(\eta_\mathrm{f} \le 0.03\,\mathrm{Pa{\cdot}s}) \tag{11}$$

and

$$\frac{v_\mathrm{t}}{\sqrt{dg}} = 0.065\left(\frac{y}{d}\right) + 0.074$$

$$(R^2 = 0.960)\ \textit{DEM}\,(\eta_\mathrm{f} = 0.22\,\mathrm{Pa{\cdot}s}) \tag{12}$$

However, for the largest viscosity data ($\eta_\mathrm{f} = 0.22$ Pa·s), deviations in the scaling between PEPT and DEM were observed. Despite this exception, the correlation between measurement and simulation was largely independent of viscosity for $\eta_\mathrm{f} \le 0.03$ Pa·s. This implies that the same constitutive equation can effectively describe both the PEPT and DEM data within this viscosity range.

Similar phenomena have been observed in other studies. Orpe and Khakhar (2001) conducted experiments on granular flow in rotating cylinders and found that the scaled velocity profiles were consistent across different materials and conditions, supporting the use of a unified constitutive framework. Brewster (2005) investigated cohesive granular flows and developed an adapted Bagnold constitutive relation. This model incorporates not only the typical collisional momentum transfer between particles but also the momentum transfer resulting from cohesive forces acting through prolonged contacts between grains during flow. Savage (1998) developed a theory for slow, dense flows of cohesionless granular materials using constitutive equations to predict the velocity and stress profiles in vertical

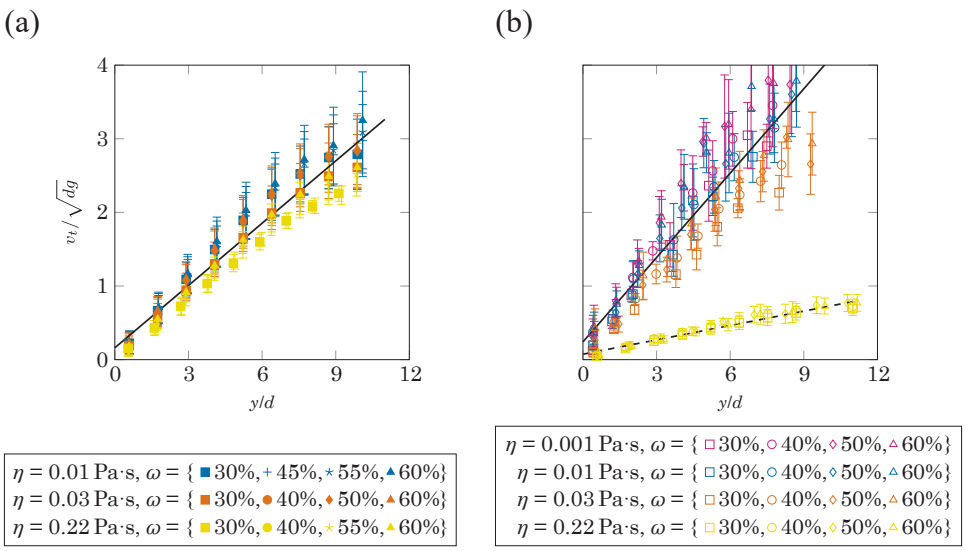

Fig. 4 Mean scaled tangential velocity, $v_\mathrm{t} / \sqrt{dg}$ at various points along perpendicular slices of the flowing layer for **(a)** PEPT (drum speeds listed in **Table 2**) and **(b)** DEM (drum speeds listed in **Table 1**) (adapted with permission from De Klerk, 2019). The raw data are publicly available at J-STAGE Data (https://doi.org/10.50931/data.kona.28792256).

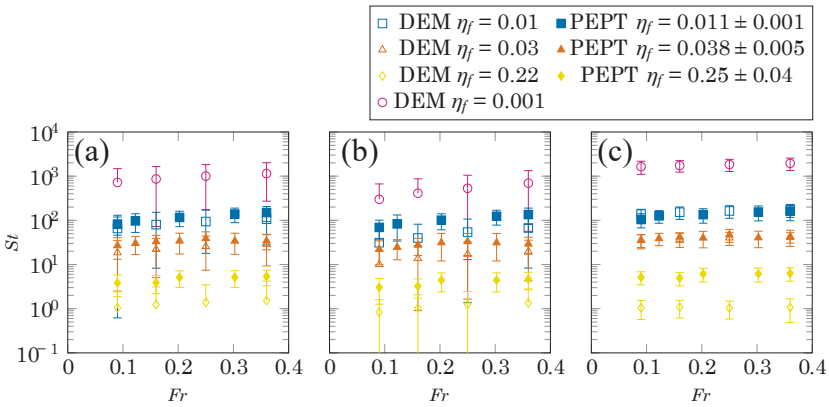

Fig. 5 *St* (*Fr*) for **(a)** all bed locations, **(b)** rising region, and **(c)** flowing layer (adapted with permission from De Klerk, 2019). The raw data are publicly available at J-STAGE Data (https://doi.org/10.50931/data.kona.28792256).

chute flows.

In **Fig. 5** the relationship between average Stokes (*St*) and Froude (*Fr*) numbers is explored for different bed locations. The agreement between PEPT and DEM was generally good, except for $\eta_f = 0.22$ Pa·s, where the lubrication approximation underestimates the *St* number. Falkovich and Pumir (2004) studied the distribution of heavy particles in turbulent flows, focusing on the dependence of particle concentration on Reynolds, Stokes, and Froude numbers. The research emphasised the discrepancies in the theoretical predictions at varying Froude numbers, thus supporting the need for improved modelling approaches for high-viscosity scenarios. Owolabi et al. (2024) investigated the turbulence modulation by large heavy particles in wall-bounded flows, examining a wide range of Stokes and Froude numbers. The results of this study highlight the influence of particle-induced stresses and the need for accurate parameterisation of forces, such as drag and buoyancy, at high viscosities. Morris et al. (2017) compared the lubrication approximation and Navier–Stokes CFD solutions for dam-break flows in thin films and observed that the lubrication approximation is robust for low Reynolds and Froude numbers but may underestimate effects at higher viscosities.

5. Conclusions

The intricate rheological behaviour of dense granular systems relies on dynamic microscale properties such as stress and force. In the absence of *in situ* measurement methods, numerical approaches are essential to obtain such information. However, the inherent complexities of numerical methods introduce a trade-off between computational efficiency and fidelity. The lubrication approximation effectively captures particle physics without the need for additional degrees of freedom to simulate the fluid phase in high Stokes regimes.

In this study, a lubrication approximation was used to model the viscous effects in a thin fluid film between particles. A comparison between DEM simulations and PEPT measurements was made for a granular suspension within a rotating drum geometry. The fluid viscosity values of $\eta_f = 0.01,0.03,0.22$ Pa·s were evaluated at drum speeds corresponding to $Fr = [0.09,0.36]$ and $St \sim [1,1000]$.

The scaled tangential velocity profiles and the range of *St* numbers showed decent agreement between the DEM simulations and the PEPT measurements, except at the highest viscosity $\eta_f = 0.22$ Pa·s. The results suggest that the lubrication approximation adequately models the effect of interstitial fluids on granular materials in high Stokes regimes. This is achieved by introducing an additional particle–particle force, which simplifies the mathematical representation and reduces the computational load. For $\eta_f = 0.22$ Pa·s, viscosity parametrisation should be investigated to evaluate whether a consistent tuning can be applied to achieve satisfactory agreement between the DEM simulations and PEPT measurements.

This study establishes the applicability of the same constitutive equation to model PEPT and DEM data within a specified viscosity range, with deviations at higher viscosities. This insight is vital for understanding the dynamics of the flowing layer, and refining simulation parameters is vital for accurate prediction.

Acknowledgments

The authors acknowledge the University of Cape Town's ICTS High Performance Computing Centre (hpc.uct.ac.za) for providing computational resources. Additionally, gratitude is extended to iThemba LABS for facilitating access to the PEPT laboratory (peptcapetown.uct.ac.za).

Data Availability Statement

The data on the viscosity in DEM simulations for complex flow regimes are available publicly in J-STAGE Data (https://doi.org/10.50931/data.kona.28792256).

References

Amarsid L., Delenne Y.-J., Mutabaruka P., Monerie Y., Perales F., Radjai F., Viscoinertial regime of immersed granular flows, Physical Review E, 96 (2017) 012901. https://doi.org/10.1103/PhysRevE.96.012901

Apostolou K., Hrymak A.N., Discrete element simulation of liquid-particle flows, Computers & Chemical Engineering, 32 (2008) 841–856. https://doi.org/10.1016/j.compchemeng.2007.03.018

Artoni R., Richard P., Average balance equations, scale dependence, and energy cascade for granular materials, Physical Review E, 91 (2015) 032202. https://doi.org/10.1103/PhysRevE.91.032202

Babic M., Average balance equations for granular materials, International Journal of Engineering Science, 35 (1997) 523–548. https://doi.org/10.1016/S0020-7225(96)00094-8

Ball R.C., Melrose J.R., A simulation technique for many spheres in quasi-static motion under frame-invariant pair drag and Brownian forces, Physica A: Statistical Mechanics and its Applications, 347 (1997) 444–472. https://doi.org/10.1016/S0378-4371(97)00412-3

Bemrose C.R., Fowles P., Hawkesworth M.R., O'Dwyer M.A., Application of positron emission tomography to particulate flow measurement in chemical engineering processes, Nuclear Instruments and Methods in Physics Research Section A: Accelerators, Spectrometers, Detectors and Associated Equipment, 273 (1988) 874–880. https://doi.org/10.1016/0168-9002(88)90111-8

Bolton G.R., LaCasse D., Lazzara M.J., Kuriyel R., The fiber-coating model of biopharmaceutical depth filtration, AIChE Journal, 51 (2005) 2978–2987. https://doi.org/10.1002/aic.10541

Brilliantov N.V., Spahn F., Hertzsch J.-M., Pöschel T., Model for collisions in granular gases, Physical Review E, 53 (1996) 5382–5392. https://doi.org/10.1103/PhysRevE.53.5382

Boyer F., Guazzelli É., Pouliquen O., Unifying suspension and granular rheology, Physical Review Letters, 107 (2011) 188301. https://doi.org/10.1103/PhysRevLett.107.188301

Brewster R., Grest G.S., Landry J.W., Levine A.J., Plug flow and the breakdown of Bagnold scaling in cohesive granular flows, Physical Review E, 72 (2005) 061301. https://doi.org/10.1103/PhysRevE.72.061301

Cai W., Effect of particle packing on flow property and strength of concrete mortar, PhD thesis, Iowa State University (2017). https://dr.lib.iastate.edu/bitstreams/50c9b70c-9054-4c6a-8590-a8baee03e379/download

Chen Y., Jin G, Zhang P., Galindo-Torres S.A., Scheuermann A., Li L., Intercomparison of boundary schemes in lattice boltzmann method for flow simulation in porous media, International Journal for Numerical Methods in Fluids, 92 (2020) 2009–2029. https://doi.org/10.1002/fld.4858

Cheng N.-S., Formula for the viscosity of a glycerol−water mixture, Industrial & Engineering Chemistry Research, 47 (2008) 3285–3288. https://doi.org/10.1021/ie071349z

Chou H.-T., Lee C.-F., Cross-sectional and axial flow characteristics of dry granular material in rotating drums, Granular Matter, 11 (2009) 13–32. https://doi.org/10.1007/s10035-008-0118-y

Cleary P.W., Delaney G.W., Sinnott M.D., Morrison R.D., Inclusion of incremental damage breakage of particles and slurry rheology into a particle scale multiphase model of a SAG mill, Minerals Engineering, 128 (2018a) 92–105. https://doi.org/10.1016/J.MINENG.2018.08.026

Cleary P.W., Morrison R.D., Delaney G.W., Incremental damage and particle size reduction in a pilot SAG mill: DEM breakage method extension and validation, Minerals Engineering, 128 (2018b) 56–68. https://doi.org/10.1016/J.MINENG.2018.08.021

Cleary P.W., Sinnott M.D., Morrison R.D., Prediction of slurry transport in SAG mills using SPH fluid flow in a dynamic DEM based porous media, Minerals Engineering, 19 (2006) 1517–1527. https://doi.org/10.1016/J.MINENG.2006.08.018

Cole K.E., Buffler A., Van der Meulen N.P., Cilliers A.A., Franzidis J.-P., Govender I., Liu C., Van Heerden M.R., Positron emission particle tracking measurements with 50 micron tracers, Chemical Engineering Science, 75 (2012) 235–242. https://doi.org/10.1016/j.ces.2012.02.053

Cortet P.-P., Bonamy D., Daviaud F., Dauchot O., Dubrulle B., Renouf M., Relevance of visco-plastic theory in a multi-directional inhomogeneous granular flow, EPL Europhysics Letters, 88 (2009) 14001. https://doi.org/10.1209/0295-5075/88/14001.

Cox R.G., The motion of suspended particles almost in contact, International Journal of Multiphase Flow, 1 (1974) 343–371. https://doi.org/10.1016/0301-9322(74)90019-6

Coussot P., Nguyen Q.D., Huynh H.T., Bonn D., Viscosity bifurcation in thixotropic, yielding fluids, Journal of Rheology, 46 (2002) 573–589. https://doi.org/10.1122/1.1459447

Cui K.F.E., Zhou G.G.D., Jing L., Viscous effects on the particle size segregation in geophysical mass flows: Insights from immersed granular shear flow simulations, Journal of Geophysical Research: Solid Earth, 126 (2021) e2021JB022274. https://doi.org/10.1029/2021JB022274

Cundall P.A., Strack O.D.L., A discrete numerical model for granular assemblies, Géotechnique, 29 (1979) 47–65. https://doi.org/10.1680/geot.1979.29.1.47

De Klerk D.N., Investigating multi-directional inhomogeneous granular suspensions, PhD thesis, University of Cape Town (2019). http://hdl.handle.net/11427/31229

El-Emam M.A., Zhou L., Shi W., Han C., Bai L., Agarwal R., Theories and applications of CFD–DEM coupling approach for granular flow: a review, Archives of Computational Methods in Engineering, 28 (2021) 4979–5020. https://doi.org/10.1007/s11831-021-09568-9

Falkovich G., Pumir A., Intermittent distribution of heavy particles in a turbulent flow, Physics of Fluids, 16 (2004) L47–L50. https://doi.org/10.1063/1.1755722

Gladkyy A., Schwarze R., Comparison of different capillary bridge models for application in the discrete element method, Granular Matter, 16 (2014) 911–920. https://doi.org/10.1007/s10035-014-0527-z

Glasser B.J., Goldhirsch I., Scale dependence, correlations, and fluctuations of stresses in rapid granular flows, Physics of Fluids, 13 (2001) 407–420. https://doi.org/10.1063/1.1338543.

Govender I., Richter M.C., Mainza A.N., De Klerk D.N., A positron emission particle tracking investigation of the scaling law governing free surface flows in tumbling mills, AIChE Journal, 63 (2017) 903–913. https://doi.org/10.1002/aic.15453.

Guo Y., Curtis J.S., Discrete element method simulations for complex granular flows, Annual Review of Fluid Mechanics, 47 (2015) 21–46. https://doi.org/10.1146/annurev-fluid-010814-014644

Guo Z., Zhao T.Z, Lattice boltzmann model for incompressible flows through porous media, Physical Review E, 66 (2002) 036304. https://doi.org/10.1103/PhysRevE.66.036304

Hawkesworth M.R., O'Dwyer M.A., Walker J., Fowles P., Heritage J., Stewart P.A.E., Witcomb R.C., Bateman J.E., Connolly J.F., Stephenson R., A positron camera for industrial application, Nuclear Instruments and Methods in Physics Research Section A: Accelerators, Spectrometers, Detectors and Associated Equipment, 253 (1986) 145–157. https://doi.org/10.1016/0168-9002(86)91138-1

Hu H.H., Joseph D.D., Crochet M.J., Direct simulation of fluid particle motions, Theoretical and Computational Fluid Dynamics, 3 (1992) 285–306. https://doi.org/10.1007/BF00717645

Jop P., Rheological properties of dense granular flows, Comptes Rendus Physique, 16 (2015) 62–72. https://doi.org/10.1016/j.crhy.2014.12.001

Jop P., Forterre Y., Pouliquen O., Crucial role of sidewalls in granular surface flows: consequences for the rheology, Journal of Fluid Mechanics, 541 (2005) 167–192. https://doi.org/10.1017/S0022112005005987

Kan H., Nakamura H., Watano S., Numerical simulation of particle–particle adhesion by dynamic liquid bridge, Chemical Engineering Science, 138 (2015) 607–615. https://doi.org/10.1016/j.ces.2015.08.043

Kim S., Karrila S.J., Microhydrodynamics, Butterworth-Heinemann, 1991, ISBN: 978-0-7506-9173-4. https://doi.org/10.1016/C2013-0-04644-0

Kloss C., Goniva C., Hager A., Amberger S., Pirker S., Models, algorithms and validation for opensource DEM and CFD-DEM, Progress in Fluid Dynamics, An International Journal, 12 (2012) 140–152.

https://doi.org/10.1504/PCFD.2012.047457
Lin S.-Y., Chen Y.-C., A pressure correction-volume of fluid method for simulations of fluid–particle interaction and impact problems, International Journal of Multiphase Flow, 49 (2013) 31–48. https://doi.org/10.1016/j.ijmultiphaseflow.2012.09.003
Liu G.R., Liu M.B., Smoothed Particle Hydrodynamics: A Meshfree Particle Method, World Scientific Publishing Company, 2003, ISBN: 9789812564405. https://doi.org/10.1142/5340
Malahe M., A one-way coupled DEM-CFD scheme to mode free-surface flows in tumbling mills, masters thesis, University of Cape Town, 2012. http://hdl.handle.net/11427/10792
Marzougui D., Chareyre B., Chauchat J., Microscopic origins of shear stress in dense fluid–grain mixtures, Granular Matter, 17 (2015) 297–309. https://doi.org/10.1007/s10035-015-0560-6
Mayank K., Malahe M., Govender I., Mangadoddy N., Coupled DEM-CFD model to predict the tumbling mill dynamics, Procedia IUTAM, 15 (2015) 139–149. https://doi.org/10.1016/j.piutam.2015.04.020
Macaulay M., Rognon P., Viscosity of cohesive granular flows, Soft Matter, 17 (2021) 165–173. https://doi.org/10.1039/D0SM01456G
Morris S., Sellier M., Behadili A.R.A., Comparison of lubrication approximation and Navier-Stokes solutions for dam-break flows in thin films, arXiv preprint, (2017) arXiv:1708.00976. https://doi.org/10.48550/arXiv.1708.00976
Moodley T.L., Govender I., Experimental validation of DEM in rotating drums using positron emission particle tracking, Mechanics Research Communications, 121 (2022) 103861. https://doi.org/10.1016/j.mechrescom.2022.103861
Ness C., Sun J., Flow regime transitions in dense non-Brownian suspensions: rheology, microstructural characterization, and constitutive modeling, Physical Review E, 91 (2015) 12201. https://doi.org/10.1103/PhysRevE.91.012201
Ness C., Sun J., Shear thickening regimes of dense non-Brownian suspensions, Soft Matter, 12 (2016) 914–924. https://doi.org/10.1039/C5SM02326B
Owolabi B., Jäckel R., Moriconi L., Loureiro J., Turbulence modulation by large heavy particles in wall-bounded turbulence, Proceedings of the International Symposium on the Application of Laser and Imaging Techniques to Fluid Mechanics, 21 (2024). https://doi.org/10.55037/lxlaser.21st.172
Orpe A.V., Khakhar D.V., Scaling relations for granular flow in quasi-two-dimensional rotating cylinders, Physical Review E, 64 (2001) 031302. https://doi.org/10.1103/PhysRevE.64.031302
Pähtz T., Durán O., De Klerk D.N., Govender I., Trulsson M., Local rheology relation with variable yield stress ratio across dry, wet, dense, and dilute granular flows, Physical Review Letters, 123 (2019) 048001. https://doi.org/10.1103/PhysRevLett.123.048001
Parker D.J., Broadbent C.J., Fowles P., Hawkesworth M.R., McNeil P., Positron emission particle tracking—a technique for studying flow within engineering equipment, Nuclear Instruments and Methods in Physics Research Section A: Accelerators, Spectrometers, Detectors and Associated Equipment, 326 (1993) 592–607. https://doi.org/10.1016/0168-9002(93)90864-E
Peters B., Baniasadi M., Baniasadi M., Besseron X., Donoso E.A., Mohseni M., Pozzetti G., XDEM multi-physics and multi-scale simulation technology: review of DEM–CFD coupling, methodology and engineering applications, Particuology, 44 (2019) 176–193. https://doi.org/10.1016/j.partic.2018.04.005
Pignatel F., Asselin C., Krieger L., Christov I.C., Ottino J.M., Lueptow R.M., Parameters and scalings for dry and immersed granular flowing layers in rotating tumblers, Physical Review E, 86 (2012) 011304. https://doi.org/10.1103/PhysRevE.86.011304
Plimpton S., Fast parallel algorithms for short-range molecular dynamics, Journal of Computational Physics, 117 (1995) 1–19. https://doi.org/10.1006/jcph.1995.1039
Potapov A.V., Hunt M.L., Campbell C.S. Liquid–solid flows using smoothed particle hydrodynamics and the discrete element method, Powder Technology, 116 (2001) 204–213. https://doi.org/10.1016/S0032-5910(00)00395-8
Povall T.M., Govender I., McBride A.T., Dense granular flows in rotating drums: a computational investigation of constitutive equations, Powder Technology, 393 (2021) 238–249. https://doi.org/10.1016/j.powtec.2021.07.051
Savage S.B., Analyses of slow high-concentration flows of granular materials, Journal of Fluid Mechanics, 377 (1998) 1–26. https://doi.org/10.1017/S0022112098002936
Seto R., Mari R., Morris J.F., Denn M.M., Discontinuous shear thickening of frictional hard-sphere suspensions, Physical Review Letters, 111 (2013) 218301. https://doi.org/10.1103/PhysRevLett.111.218301
Silbert L.E., Landry J.W., Grest G.S., Granular flow down a rough inclined plane: transition between thin and thick piles, Physics of Fluids, 15 (2003) 1–10. https://doi.org/10.1063/1.1521719
Sun R., Xiao H., SediFoam: a general-purpose, open-source CFD–DEM solver for particle-laden flow with emphasis on sediment transport, Computers & Geosciences, 89 (2016) 207–219. https://doi.org/10.1016/J.CAGEO.2016.01.011
Tanaka T., Kawaguchi T., Tsuji Y., Discrete particle simulation of flow patterns in two-dimensiona gas fluidized beds, International Journal of Modern Physics B, 07 (1993) 1889–1898. https://doi.org/10.1142/S0217979293002663
Tichy J.A., A surface layer model for thin film lubrication, Tribology Transactions, 38 (1995) 577–582. https://doi.org/10.1080/10402009508983445
Trulsson M., Andreotti B., Claudin P., Transition from the viscous to inertial regime in dense suspensions, Physical Review Letters, 109 (2012) 118305. https://doi.org/10.1103/PhysRevLett.109.118305
Tsuji Y., Kawaguchi T., Tanaka T., Discrete particle simulation of two-dimensional fluidized bed, Powder Technology, 77 (1993) 79–87. https://doi.org/10.1016/0032-5910(93)85010-7
Wang T., Zhang F., Furtney J., Damjanac B., A review of methods, applications and limitations for incorporating fluid flow in the discrete element method, Journal of Rock Mechanics and Geotechnical Engineering, 14 (2022) 1005–1024. https://doi.org/10.1016/j.jrmge.2021.10.015
Washino K., Chan E.L., Midou H., Tsuji T., Tanaka T., Tangential viscous force models for pendular liquid bridge of newtonian fluid between moving particles, Chemical Engineering Science, 174 (2017) 365–373. https://doi.org/10.1016/j.ces.2017.09.028
Washino K., Tan H.S., Hounslow M.J., Salman A.D., A new capillary force model implemented in micro-scale CFD–DEM coupling for wet granulation, Chemical Engineering Science, 93 (2013) 197–205. https://doi.org/10.1016/j.ces.2013.02.006
Wildmann R.D., Huntley J.M., Hansen J.-P., Parker D.J., Allen D.A., Single-particle motion in three dimensional vibrofluidised beds, Physical Review E, 62 (2000) 3826–3835. https://doi.org/10.1103/PhysRevE.62.3826
Xiao H., Sun J., Algorithms in a robust hybrid CFD-DEM solver for particle-laden flows, Communications in Computational Physics, 9 (2011) 297–323. https://doi.org/10.4208/cicp.260509.230210a.
Yang G.C., Jing L., Kwok C.Y., Sobral Y.D., A comprehensive parametric study of LBM-DEM for immersed granular flows, Computers and Geotechnics, 114 (2019) 103100. https://doi.org/10.1016/j.compgeo.2019.103100
Zhu H.P., Zhou Z.Y., Yang R.Y., Yu A.B., Discrete particle simulation of particulate systems: theoretical developments, Chemical Engineering Science, 62 (2007) 3378–3396. https://doi.org/10.1016/j.ces.2006.12.089
Zhu H.P., Zhou Z.Y., Yang R.Y., Yu A.B., Discrete particle simulation of particulate systems: a review of major applications and findings, Chemical Engineering Science, 63 (2008) 5728–5770. https://doi.org/10.1016/j.ces.2008.08.006
Zhu R., LI S., Yao Q., Effect of cohesion on granular-fluid flows in spouted beds: PIV measurement and DEM simulations, AIP Conference Proceedings, 1542 (2013) 979–982. https://doi.org/10.1063/1.4812097

Authors' Short Biographies

Dr. David de Klerk has a background in physics and computer science. He has more than two decades of programming and software development experience, with a focus on scientific computing. His PhD topic was granular flow in the context of mineral processing and comminution using computer simulations and experimental techniques.

Prof. Indresan Govender is Group Executive: Mineral Processing & Characterisation (MPC) at Mintek. With over 20 years of R&D experience, he brings to Mintek a strong track record that spans the full value chain of mineral processing research. The goal of the MPC cluster is to integrate data, technology and modelling to gain insights into the location, quantity, liberation, and economic viability of mineral deposits. The broad range of research skills underpinning the MPC cluster are central to this goal.

Dr. Taswald Moodley is a Principal Engineer at Mintek and an Honorary Research Fellow at the University of KwaZulu-Natal. With nearly 15 years of research and development experience, his work focuses on the simulation of minerals processing systems (using DEM and SPH) and their experimental validation (via PEPT). Dr. Moodley is a registered Professional Engineer (ECSA) and an active member of the Southern African Institute for Mining and Metallurgy (SAIMM).

Prof. Aubrey Mainza is Deputy Director and Head of Comminution and Classification at the Centre for Minerals Research, which is housed in the department of chemical engineering at the University of Cape Town. He has more than 25 years of experience in comminution and classification and has participated in several mineral processing plant design and plant optimisation projects around the world. He has participated in many international mineral processing projects, including the AMIRA P9 project. He is a member of the European/African editorial board of the KONA Powder and Particle Journal and sits on the international advisory board of the European Symposium on Comminution and Classification. He is a founding member of the Global Comminution Collaborative and a consultant for the Minerals Engineering International Comminution Conference. He is also a member of the International Minerals Processing Congress Board.